

Shot noise suppression and hopping conduction in graphene nanoribbons

R. Danneau,^{1,2,*} F. Wu,^{1,†} M. Y. Tomi,¹ J. B. Oostinga,³ A. F. Morpurgo,³ and P. J. Hakonen¹

¹Low Temperature Laboratory, Aalto University, P.O. Box 13500, FI-00076 AALTO, Finland

²Institute of Nanotechnology, Karlsruhe Institute of Technology, D-76021 Karlsruhe, Germany
and Institute of Physics, Karlsruhe Institute of Technology, D-76128 Karlsruhe, Germany

³DPMC and GAP, University of Geneva, quai Ernest-Ansermet 24, CH-1211 Geneve, Switzerland

(Received 22 May 2010; revised manuscript received 13 September 2010; published 7 October 2010)

We have investigated shot noise and conduction of graphene field-effect nanoribbon devices at low temperature. By analyzing the exponential I - V characteristics of our devices in the transport gap region, we found out that transport follows variable range hopping laws at intermediate bias voltages $1 < V_{bias} < 12$ mV. In parallel, we observe a strong shot noise suppression leading to very low Fano factors. The strong suppression of shot noise is consistent with inelastic hopping, in crossover from one- to two-dimensional regime, indicating that the localization length $l_{loc} < W$ in our nanoribbons.

DOI: [10.1103/PhysRevB.82.161405](https://doi.org/10.1103/PhysRevB.82.161405)

PACS number(s): 72.80.Vp, 73.50.Td

Graphene, a two-dimensional crystal of carbon atoms, has attracted a tremendous interest of both scientific community and microelectronic industry.¹ However, graphene is a zero-gap semiconductor with a minimum conductivity of $4e^2/\pi h$ too large to be utilized as base material for high on-off ratio field-effect transistor. One way to circumvent this problem would be to open a gap in graphene's band structure. It is possible in bilayer graphene by the means of doping (either chemical² or electrostatic³). Another way to create an efficient graphene transistor is to build a constriction and/or to form a nanoribbon. Early theoretical studies have predicted that a gap could be opened in graphene nanoribbons (GNR) depending on the edges being either zigzag or armchair.⁴

However, the first studies of GNRs were performed on etched graphene leading to ribbon width down to around 20 nm.^{5,6} These experiments demonstrated the presence of a transport gap inversely proportional to the width and independent on the crystallographic orientation.⁶ It was also estimated that part of the ribbons at the edges were probably not conducting (around 14 nm at $T=4.2$ K), suggesting that edge roughness is significant. Similar transport gaps were observed for much smaller ribbon width in GNRs fabricated using sonication of intercalated graphite in solution, indicating smoother edges than the etched GNRs.⁷ Indeed, experiments performed on GNRs (Refs. 5, 6, and 8–10) tend to prove that the origin of the gap may be more complex than the early theoretical studies suggested.⁴ Despite several models based on Anderson localization, Coulomb blockade, or percolation phenomenon,¹¹ there is not yet a consensus as to the origin of the gap in GNRs.

In this work, we report the shot noise measurements on etched GNRs performed at low temperature. Our results show a strong shot noise reduction while I - V characteristics measured follow variable range hopping (VRH) laws¹² in the gap region. Such a shot noise suppression is the consequence of inelastic hopping conduction from a localized state to an adjacent one, localized states arising from the rough edges and disorder due to residues and defects from the fabrication process. We also find that relaxation of electrons is stronger than expected in our ribbons.

The GNRs have been fabricated from the same graphene monolayer (identified using the RGB greenshift as described

in Refs. 3, 10, and 13) using Scotch tape micromechanical cleavage on natural graphite. The graphene sheets were deposited on a heavily p -doped substrate with 300 nm SiO_2 layer [see Fig. 1(a)]. The graphene sheet was first connected using standard e-beam lithography followed by a Ti(10 nm)/Au(40 nm) bilayer deposition with lift-off in acetone. A second lithography step allowed the patterning of the GNRs. The resist poly(methyl methacrylate) (PMMA) was used as mask in this step and GNRs were etched using an Ar plasma. We present the measurements on two GNRs: sample A with a length $L \sim 600$ nm and a nominal width $W \sim 90$ nm, and sample B with a length $L \sim 200$ nm and a nominal width $W \sim 70$ nm. After the experiments, the GNRs were observed using scanning electron microscope at 0.5 kV [see Fig. 1(b)].

The measurements were performed in a similar fashion as described in Ref. 14, from room temperature down to $T = 4.2$ K. The differential conductance $\frac{dI}{dV}$ was measured using standard low-frequency ac lock-in technique with an excitation amplitude from 0.38 mV up to 0.8 mV (~ 4 to ~ 8 K) at $f = 63.5$ Hz. A tunnel junction was used for calibration of the shot noise.^{14,15}

Figures 2(a) and 2(b) display the gate voltage V_{gate} dependence of the zero-bias conductance G for different temperatures T of sample A and B, respectively. In both cases, we observe a drop of G when T is lowered and a high impedance region emerges as $T \rightarrow 4.2$ K. Clear conductance oscillations at zero bias are visible at the lowest temperatures. However, no periodicity is detectable in a Fourier analysis. Far away

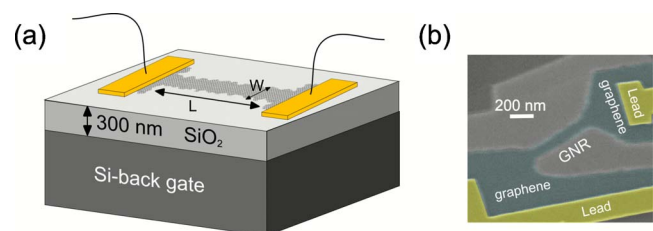


FIG. 1. (Color online) (a) Schematics of an etched GNR. (b) False color scanning electron micrograph of sample A, highlighting the graphene and the GNR (in blue/dark gray) and the leads (in yellow/light gray).

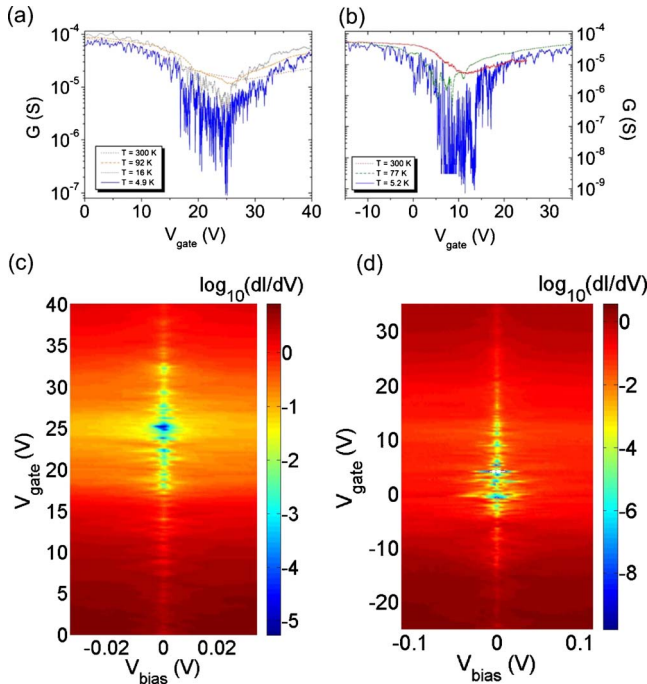


FIG. 2. (Color online) [(a) and (b)] G versus V_{gate} at various temperatures for sample A and B, respectively. [(c) and (d)] Color map of $\frac{dI}{dV}$ versus V_{bias} and V_{gate} with step of 0.2 and 0.3 V between each biasing at $T=4.9$ and 5.2 K for sample A and B, respectively.

from the charge neutrality point $G \sim 2e^2/h$, i.e., twice the conductance quantum g_0 . Figures 2(c) and 2(d) show a color map of the scaled differential conductance $\frac{dI}{dV}/g_0$ as a function of bias voltage V_{bias} and V_{gate} at liquid helium temperature, for sample A and B, respectively. These measurements highlight the formation of a “large impedance region” or a “gap” as previously observed.^{5,6,8–10} This region can be viewed in different ways. In the Anderson picture, it arises from localization due to the rough edges and the disorder resulting in to the high impedance region (around the original Dirac point) at zero bias. Out of equilibrium measurements, on the other hand, illuminate the Coulombic aspects of the transport suppression in GNRs: a “source and drain” gap is modulated by the “Coulomb diamondlike” structures which could originate from the formation of a series of dots, all contributing their share to the gap. We found “source drain gap” of about 5 meV and 15 meV from our $\frac{dI}{dV}-V_{bias}$ data and a “transport gap” of about 14 V and 18 V from the $\frac{dI}{dV}-V_{gate}$ curves for sample A and B, respectively. We observe clear irregular Coulomb diamondlike structures comparable to previous studies,^{5,6,8–10} suggesting that Coulomb interactions are significant.

VRH generally describes electronic transport in the presence of disorder.¹² Temperature dependence of the conductance $G(T)$ is conventionally used to identify the regime. In the case of GNRs, the minimum conductance can vary in gate voltage V_{gate} as the temperature is lowered even under vacuum condition,⁶ leading to uncertainties in the data analysis. The uncontrolled doping by adsorbed molecules may move the minimum conduction region during the cooldown. However, $G(T)$ study has been recently successfully

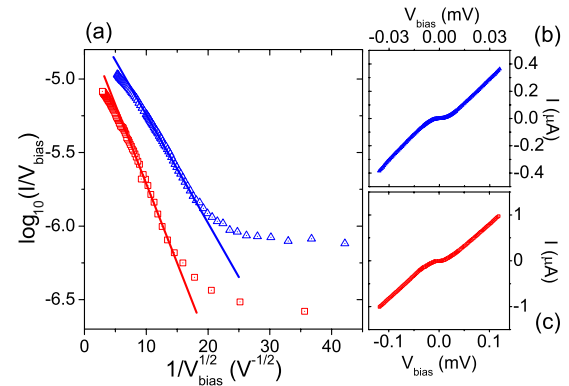


FIG. 3. (Color online) $I-V$ characteristics of sample A and B plotted using hopping law at high bias (a), Eq. (1), at $V_{gate}=25.4$ and 11 V at $T=4.9$ and 5.2 K for sample A and B, respectively (Δ and \square). The plot shows linear behavior in the log scale with $1/V_{bias}^{1/2}$ above the gap [flat part of (b) and (c)] and below V_0 , i.e., where the data starts to deviate from linear in (a). (b) and (c) are the corresponding normal $I-V$ plots of sample A and B, respectively.

performed.⁹ An alternative way is to analyze $I-V$ curves at a temperature T . At high bias, below a certain V_0 , the following equation can be used to describe VRH:¹⁶

$$I(E, T) = VG_0(T) \exp \left\{ - \left(\frac{V_0}{V} \right)^{1/(d+1)} \right\}, \quad (1)$$

where d is the dimensionality of hopping (for the effect of interactions, see below) and G_0 is the zero-bias conductance. Equation (1) transforms to Mott’s law by replacement of $eV_0 = k_B T_0$ and $eV = k_B T$ in the exponent (V_0 being the upper most value for which the formula is valid) which provides the basic motivation for using this functional form.^{17–19}

Figure 3 displays $I-V$ curves for sample A and B measured in the gap region. Following Eq. (1), we see that the conduction follows variable range hopping law in the gap region. The data are plotted using $d=1$ which describes VRH for one-dimensional (1D) systems with or without interactions or two-dimensional (2D) systems with interactions. We obtain $V_0 \sim 8$ and 12 mV for sample A and B, respectively. Here, $\frac{a}{L}eV_0$ describes the bias needed to overcome the potential barrier of the localized state with radius a . The fact that we obtain a larger V_0 for sample B which has a width 20 nm smaller (and is even shorter) than sample A indicates an enhanced influence of the rough edges on the conduction. Consequently, our results show that the appearance of the high impedance region in GNRs is also affected by defects such as localized states at the edges and, likewise, by the local doping due to contaminants. This is in agreement with the recent works on temperature dependence of GNR conductance.⁹ Han *et al.*⁹ have shown that for various GNR geometries $l \geq W$ indicating 1D VRH transport in the high impedance region of GNRs; the origin of the transport gap would then be due to localized states. This has recently been confirmed by magnetotransport measurements.¹⁰ Our value for $V_0 \approx 10$ meV is close to the value $k_B T_0 / e \approx 6$ meV given in Ref. 10.

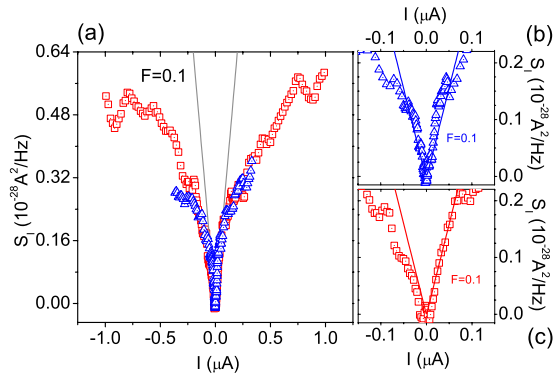


FIG. 4. (Color online) (a) S_I versus I averaged over three gate values around $V_{gate}=25.4$ V and $T=4.9$ K for sample A (Δ), and $V_{gate}=11$ V and $T=5.2$ K for sample B (\square). We show a low-bias fit for sample B using the Khlus formula with F as the only fitting parameter. F decreases at higher bias (see text). [(b) and (c)] S_I versus I zoomed in the low-bias region.

In order to gain more information on the hopping in GNRs, we have studied shot noise. Shot noise denotes current fluctuations arising from the granular nature of the charge carriers (see Ref. 20 for a review). It provides a powerful tool to probe mesoscopic systems and it is usually regarded as a complementary technique to conductance measurements. The Fano factor F , given by the ratio of shot noise and mean current, is commonly employed to quantify shot noise. The noise power spectrum then reads $S(I)=F \times 2eI$. In the case of phase-coherent transport in GNRs, shot noise strongly depends on the boundary conditions, i.e., whether the edges are zigzag or armchair.²¹ However, phase-coherent length in etched GNRs have been estimated to be at most 175 nm (Ref. 10) and it is clearly less in our experiment due to higher temperature and a finite bias that enhances energy relaxation. While in the case of phase-coherent transport, shot noise can be described simply by the scattering matrix theory, it can be treated using semiclassical means in the incoherent regime. When inelastic processes dominate (inelastic length $l_{in} < L$), shot noise starts to decrease and it becomes dependent on the details of the relaxation processes that govern the ensuing nonequilibrium state. In inelastic hopping conduction with short hopping length ($l_{hop} \ll L$), strong suppression of shot noise takes place as observed in 2D systems.²²

Assuming strongly inelastic behavior, classical addition of uncorrelated noise sources can be employed and networks of resistors with shunting current noise generators become an appealing choice for noise modeling in GNRs. Within this classical limit, the internal topology of the ribbon becomes relevant. If hopping is 2D in GNRs, then part of the noise current of individual noise generators is shunted via the conduction paths inside the ribbon and the noise coupled to an outside load becomes reduced. Consequently, we expect that the Fano factor is reduced a bit further down from the 1D classical limit given by l_{hop}/L .

We have performed our shot noise measurements at frequency around 800 MHz. This frequency is high enough so that all noise due to slow fluctuations of resistance (transmis-

sion coefficients) can be neglected. On the other hand, the frequency is low compared with internal charge relaxation-time scales and high-frequency effects can be neglected. Figure 4(a) displays the current noise per unit bandwidth S_I versus current I in the high impedance region for samples A and B, respectively. Both curves are fitted using the formula defined by Khlus²³ with F as the only fitting parameter.¹⁴ We find a rather low Fano factor for both GNRs $F \sim 0.1$ at low bias (the results involve a correction due to nonlinear I - V curves as discussed in Ref. 14). Figures 4(b) and 4(c) show a zoom of the noise curves in the low-bias region, i.e., in the VRH regime (up to $I \sim 0.05$ μ A corresponding to $V \sim 10$ mV) for sample A and B, respectively. Despite some asymmetry in the shot noise, F undergoes very little variation in the gap region.²⁴ With increasing bias, we find a further reduction in the Fano factor, which signals a strong role of inelastic processes as the localized states become delocalized.

Why such a low shot noise? The observed conductance modulation in the high impedance regime suggests that a series/array of dots is formed in GNRs. Quantum dots often show super-Poissonian noise instead of low noise level (see, for example, the work done on carbon nanotubes^{25,26}) and as theoretically expected for a series of quantum dots.²⁷ However, a series of N quantum dots without inelastic effects should lead to a Fano factor of $\frac{1}{3}$.²⁸ We note that shot noise suppression could be seen in asymmetric, open quantum cavity,²⁰ but the resistance of one or two open quantum cavities (regions at the ends of the ribbon) is too small to account for our results. There will, however, be a small contribution by the end reservoirs on the shot noise.

The main contribution to the shot noise suppression can only come from hopping conduction via so small localized states that the nature of hopping conduction is likely to be almost 2D. F for a series of N sites with inelastic hopping is approximately $1/N \sim l_{hop}/L$, and this remains as a good approximation also in the 2D situation, where N then denotes the number of hops along the voltage bias. In order to explain the observed suppression, the hopping length has to be in the range of $l_{hop} \sim 20$ – 60 nm; as the localization length $l_{loc} \sim l_{hop}$ is less than the width of the GNR, we conclude that the hopping conduction in our ribbons is not 1D in nature but rather it falls in the crossover regime between 1D and 2D (or quasi-1D). Our shot noise results thus indicate even a slightly smaller l_{hop} than was found previously.^{9,10}

The shot noise crossover from VRH region to high-bias regime without localized states in Fig. 4 points to strong relaxation of electrons: otherwise an increase in the Fano factor would be expected across the crossover as the number of hops decreases and l_{loc} increases.^{18,22} Indeed, even in the VRH regime, the apparent Fano factor could be formed by other means, for example, by noise from the graphene islands at the ends, and that the actual shot noise from the GNR nearly vanishes. This would be reminiscent to carbon nanotubes where very small F have been observed in various configurations.^{29,30} Nearly total suppression of shot noise indicates very effective energy relaxation at finite bias which

could be realized by disorder-enhanced electron-phonon coupling³¹ or by relaxation via new degrees of freedom provided by the edges of the GNR.

To conclude, we have measured shot noise and conductance in GNRs. While the dc transport shows characteristic behavior of GNRs, we clearly observe a strong shot noise suppression. We were able to fit the I - V curves with VRH laws in the high impedance region. We have shown that shot noise suppression could be explained by inelastic hopping conduction in the quasi-1D limit. Our results are consistent with the strong effect of rough edges and local contaminants in the conduction and shot noise of GNRs.

We thank F. Evers, D. Golubev, T. Heikkilä, M. Hettler, A. Iosevich, P. Pasanen, M. Laakso, G. Metalidis, and M. Paalanen for fruitful discussions and B. Shklovskii for attracting our attention to Ref. 16. R.D.'s Shared Research Group SRG 1-33 received financial support by the "Concept for the future" of the Karlsruhe Institute of Technology within the framework of the German Excellence Initiative. The work of A.F.M. is supported by SNF (Grant No. 200021-121569) and MaNEP. This work was funded by the Academy of Finland, by EU Commission (Grant No. FP6-IST-021285-2) and by Nokia NRC (NANOSYSTEMS project).

*Corresponding author; romain.danneau@kit.edu

†Present address: Microtechnology and Nanoscience MC2, Chalmers University of Technology, 41296 Göteborg, Sweden.

¹A. H. Castro Neto *et al.*, *Rev. Mod. Phys.* **81**, 109 (2009); N. M. R. Peres, *ibid.* **82**, 2673 (2010); S. Das Sarma, S. Adam, E. Hwang, and E. Rossi, arXiv:1003.4731 (unpublished).

²T. Ohta *et al.*, *Science* **313**, 951 (2006).

³J. B. Oostinga *et al.*, *Nature Mater.* **7**, 151 (2008).

⁴K. Nakada, M. Fujita, G. Dresselhaus, and M. S. Dresselhaus, *Phys. Rev. B* **54**, 17954 (1996).

⁵Z. Chen *et al.*, *Physica E* **40**, 228 (2007).

⁶M. Y. Han, B. Özyilmaz, Y. Zhang, and P. Kim, *Phys. Rev. Lett.* **98**, 206805 (2007).

⁷X. Li *et al.*, *Science* **319**, 1229 (2008); X. Wang, Y. Ouyang, X. Li, H. Wang, J. Guo, and H. Dai, *Phys. Rev. Lett.* **100**, 206803 (2008); J. M. Pomirol, A. Cresti, S. Roche, W. Escoffier, M. Goiran, X. Wang, X. Li, H. Dai, and B. Raquet, *Phys. Rev. B* **82**, 041413(R) (2010).

⁸B. Özyilmaz *et al.*, *Appl. Phys. Lett.* **91**, 192107 (2007); K. Todd *et al.*, *Nano Lett.* **9**, 416 (2009); C. Stampfer, J. Güttinger, S. Hellmüller, F. Molitor, K. Ensslin, and T. Ihn, *Phys. Rev. Lett.* **102**, 056403 (2009); F. Molitor, A. Jacobsen, C. Stampfer, J. Güttinger, T. Ihn, and K. Ensslin, *Phys. Rev. B* **79**, 075426 (2009); X. Liu, J. B. Oostinga, A. F. Morpurgo, and L. M. K. Vandersypen, *Phys. Rev. B* **80**, 121407(R) (2009); P. Gallagher, K. Todd, and D. Goldhaber-Gordon, *Phys. Rev. B* **81**, 115409 (2010).

⁹M. Y. Han, J. C. Brant, and P. Kim, *Phys. Rev. Lett.* **104**, 056801 (2010).

¹⁰J. B. Oostinga, B. Sacépé, M. F. Craciun, and A. F. Morpurgo, *Phys. Rev. B* **81**, 193408 (2010).

¹¹Y.-W. Son, M. L. Cohen, and S. G. Louie, *Phys. Rev. Lett.* **97**, 216803 (2006); D. Gunlycke, D. A. Areshkin, and C. T. White, *Appl. Phys. Lett.* **90**, 142104 (2007); F. Sols, F. Guinea, and A. H. Castro Neto, *Phys. Rev. Lett.* **99**, 166803 (2007); A. Lherbier, B. Biel, Y.-M. Niquet, and S. Roche, *ibid.* **100**, 036803 (2008); D. Querlioz *et al.*, *Appl. Phys. Lett.* **92**, 042108 (2008); S. Adam, S. Cho, M. S. Fuhrer, and S. Das Sarma, *Phys. Rev. Lett.* **101**, 046404 (2008); M. Evaldsson, I. V. Zozoulenko, H. Xu, and T. Heinzl, *Phys. Rev. B* **78**, 161407(R) (2008); I. Martin and Y. M. Blanter, *ibid.* **79**, 235132 (2009).

¹²B. I. Shklovskii and A. L. Efros, *Electronic Properties of Doped Semiconductors* (Springer-Verlag, Berlin, 1984).

¹³M. F. Craciun *et al.*, *Nat. Nanotechnol.* **4**, 383 (2009).

¹⁴R. Danneau, F. Wu, M. F. Craciun, S. Russo, M. Y. Tomi, J. Salmilehto, A. F. Morpurgo, and P. J. Hakonen, *Phys. Rev. Lett.* **100**, 196802 (2008); *J. Low Temp. Phys.* **153**, 374 (2008); *Solid State Commun.* **149**, 1050 (2009).

¹⁵F. Wu *et al.*, in *Low Temperature Physics*, AIP Conf. Proc. No. 850 (AIP, New York, 2006), p. 1482.

¹⁶B. I. Shklovskii, *Sov. Phys. Semicond.* **6**, 1964 (1973).

¹⁷M. Pollak and I. Riess, *J. Phys. C* **9**, 2339 (1976).

¹⁸Y. A. Kinkhabwala, V. A. Sverdlov, and K. K. Likharev, *J. Phys.: Condens. Matter* **18**, 2013 (2006).

¹⁹A. S. Rodin and M. M. Fogler, *Phys. Rev. B* **80**, 155435 (2009).

²⁰Ya. Blanter and M. Büttiker, *Phys. Rep.* **336**, 1 (2000).

²¹A. Cresti, G. Grosso, and G. P. Parravicini, *Phys. Rev. B* **76**, 205433 (2007); E. R. Mucciolo, A. H. Castro Neto, and C. H. Lewenkopf, *ibid.* **79**, 075407 (2009); R. L. Dragomirova, D. A. Redskin, and B. K. Nikolic, *ibid.* **79**, 241401(R) (2009).

²²V. V. Kuznetsov, E. E. Mendez, X. Zuo, G. L. Snider, and E. T. Croke, *Phys. Rev. Lett.* **85**, 397 (2000); S. H. Roshko *et al.*, *Physica E* **12**, 861 (2002); F. E. Camino, V. V. Kuznetsov, E. E. Mendez, M. E. Gershenson, D. Reuter, P. Schafmeister, and A. D. Wieck, *Phys. Rev. B* **68**, 073313 (2003); A. K. Savchenko *et al.*, *Phys. Status Solidi B* **241**, 26 (2004).

²³V. A. Khlus, *Zh. Eksp. Teor. Fiz.* **93**, 2179 (1987) [*Sov. Phys. JETP* **66**, 1243 (1987)].

²⁴It is important to note that even stronger asymmetries in the noise power spectra curves have been measured in 2D systems in the VRH regime, see Ref. 22.

²⁵E. Onac, F. Balestro, B. Trauzettel, C. F. J. Lodewijk, and L. P. Kouwenhoven, *Phys. Rev. Lett.* **96**, 026803 (2006).

²⁶F. Wu, T. Tsuneta, R. Tarkiainen, D. Gunnarsson, T.-H. Wang, and P. J. Hakonen, *Phys. Rev. B* **75**, 125419 (2007).

²⁷J. Aghassi *et al.*, *Appl. Phys. Lett.* **89**, 052101 (2006).

²⁸See, D. S. Golubev and A. D. Zaikin, *Phys. Rev. B* **70**, 165423 (2004).

²⁹P. E. Roche *et al.*, *Eur. Phys. J. B* **28**, 217 (2002).

³⁰T. Tsuneta *et al.*, *EPL* **85**, 37004 (2009).

³¹A. Sergeev and V. Mitin, *Phys. Rev. B* **61**, 6041 (2000).